THE JOURNAL OF PHYSICAL CHEMISTRY C LETTERS

2008, *112,* 2248−2251
Published on Web 01/31/2008

Phase-Dependent Desorption from Biphenyl-Substituted Alkanethiol Self-Assembled Monolayers Induced by Ion Irradiation

Frederik Vervaecke,[†] Sabina Wyczawska,[†] Piotr Cyganik,*[,‡] Zbigniew Postawa,[‡] Manfred Buck,[§] Roger E. Silverans,[†] Peter Lievens,[†] and Erno Vandeweert*[,†]

Laboratory of Solid State Physics and Magnetism and INPAC, Institute for Nanoscale Physics and Chemistry, K.U. Leuven, Celestijnenlaan 200D, 3001 Leuven, Belgium, Smoluchowski Institute of Physics, Jagiellonian University, ul. Reymonta 4, PL 30-059 Kraków, Poland, and EaStChem School of Chemistry, St Andrews University, North Haugh, St Andrews, KY16 9ST, United Kingdom

Received: December 28, 2007

Using laser ionization in combination with time-of-flight mass spectrometry, we have studied ion-induced desorption of neutral particles from self-assembled monolayers (SAMs) of ω-(4′-methylbiphenyl-4-yl) alkane thiols ($CH_3(C_6H_4)_2(CH_2)_nSH$, BP*n*, $n = 2, 4, 6$) formed on Au(111) substrates. Because BPn/Au(111) SAMs with $n =$ even exhibit polymorphism, the effect of purely structural changes on emission yield and fragmentation pattern could be studied without interference from changes in the chemical composition. In spite of the high energy of the primary ion beam (15 keV), the mass spectra reveal a striking sensitivity of the desorption process to rather subtle changes in the structure of the layer. Depending on the SAM structure, substantial differences in the ratio between the cleavage of the molecule−substrate and the C−S bonds are observed. For applications of SAMs as resists in ion beam lithography, the results demonstrate that well-defined removal of molecules requires exact control of the SAM structure.

Many nanotechnological applications currently under development rely on the patterned functionalization of surfaces with complex organic molecules. In this context, self-assembled monolayers (SAMs) play an important role.[1,2] SAMs can be used as ultrathin resist in electron,[3] photon,[3,4] neutral atom,[5] or ion[6] based lithography. Because of the small dimensions associated with these molecular systems, that is, an intermolecular distance of less than 1 nm and a typical thickness of about 1−2 nm, the potentially attainable resolution in lithography of SAMs is very high. Resolution is, however, only one crucial criterion. Another one of equal importance is the precise control of SAM lithographic processes, that is, complete removal of molecules or well-defined modification during irradiation. The latter focuses on processes occurring during ion irradiation of aromatic SAMs which, due to their potential application in molecular electronics,[7] are particularly attractive systems as resists for high-resolution lithography.

Generally, ion irradiation of SAMs results in emission of particles comprising neutral species, ions, electrons, and photons. The analysis of emission processes gives information on the desorption mechanism. To optimize static secondary ion mass spectrometry (SSIMS) for the analysis of thin organic films with SAMs as a model system, most of the studies on SAMs have focused on the emission of secondary ions (see ref 8 and references therein). There is, however, an inherent complexity in using emission of secondary ions as a fingerprint of processes taking place during ion irradiation of SAMs. The ionization mechanism, which leads to the emission of secondary ions, is poorly understood, in particular for complex organic systems, and strongly depends on matrix effects. In contrast, analysis of the neutral majority of emitted species allows for a more direct insight into the desorption process. Our previous studies[9−12] on the emission of neutral fragments from aromatic SAMs during irradiation using ions with kinetic energies of several kiloelectronvolts revealed that, surprisingly, only a small fraction of the molecules is ejected ballistically with high kinetic energies (∼eV) during the collision cascade that develops in the substrate upon impact of the ion. The majority of particles desorb at thermal-like energies (∼0.01 eV). To explain this thermal-like emission, we have proposed a model in which particles are released by a two-step mechanism. The first step consists of the cleavage of a substrate−molecule bond or an intramolecular bond by chemical reactions induced by reactive species created near the point of impact of the primary ion (e.g., radicals or secondary electrons). In the second step, molecular fragments created by bond scission remain trapped at the surface and after reaching thermal equilibrium evaporate slowly.

For a controlled removal of molecules, it is essential to understand what determines the efficiency of bond-breaking in a SAM upon ion irradiation and, in particular, complete removal of molecules. It has already been demonstrated by others that modification of the SAM substrate metal,[13] or the chemical group through which SAM constituents are bound to it,[14] has an impact on the complete removal of the SAM molecules by the ion beam. Experiments reported in this letter demonstrate that, surprisingly, complete removal of molecules induced by ion beams strongly depends on a relatively small reorientation

* Corresponding authors. E-mail: piotr.cyganik@uj.edu.pl (P.C.); Erno.VANDEWEERT@ec.europa.eu (E.V.).
[†] Laboratory of Solid State Physics and Magnetism and INPAC.
[‡] Jagiellonian University.
[§] St Andrews University.

10.1021/jp712133u CCC: $40.75

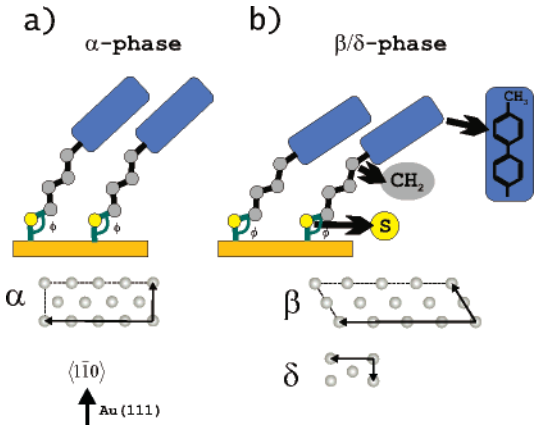

Figure 1. Schematic illustration of BPn ($CH_3(C_6H_4)_2(CH_2)_nSH$) molecules on Au(111) substrate for n = even in (a) room-temperature α phase with rectangular ($5\sqrt{3} \times 3$) structure and (b) high-temperature phases of β and δ corresponding to oblique ($6\sqrt{3} \times 2\sqrt{3}$) and rectangular ($2\sqrt{3} \times 2$) structures, respectively. Relative size and orientation of the corresponding unit cells are shown in the lower part together with the orientation of the Au(111) substrate.

of molecules in the SAMs without changes in their chemical composition. To demonstrate this effect, we have used a model aromatic system of biphenyl-based SAMs CH_3-C_6H_4-C_6H_4-$(CH_2)_n$-SH (BPn, n = 1−6) on Au(111) substrates, whose characteristics include an alkane spacer chain between the thiol group and the aromatic moiety. Previous spectroscopic[15−17] and microscopic[18,19] studies have demonstrated that the structure of the BPn/Au(111) with n = odd is pronouncedly different from the one with n = even. This odd−even effect in the film structure is reflected in a number of BPn/Au(111) film properties, for example, electrochemical stability,[20,21] stability against exchange by other thiols,[22] and stability against electron irradiation.[23] However, the most striking expression of this odd−even effect, and directly relevant for this paper, is polymorphism,[24−27] which is seen exclusively for even-numbered BPn/Au(111) SAMs. Among the variety of structures observed so far, three, labeled α, β, and δ, are of interest in the context of this paper (see Figure 1 and the Supporting Information). With access to different structures without any change in chemical composition, the even-numbered BPn/Au(111) SAMs are well-suited systems to elucidate how sensitively ion-induced scission is influenced by the film structure.

Mass spectra resulting from the ion-stimulated (15-keV Ar^+) emission of neutral, low-energy molecular fragments (0.02 eV for particles with a mass of 200 amu) from even-numbered BPn (n = 2, 4, 6) films on a Au(111) substrate are presented in Figure 2 (see the Supporting Information for experimental details). The left panel of Figure 2 shows data obtained for α-phase SAMs while the right panel displays corresponding mass spectra obtained for the β and δ phases, respectively.

Further analysis of the mass spectra of Figure 2 is based on three characteristic peaks that correspond to emission of (1) the complete molecule (CH_3-C_6H_4-C_6H_4-$(CH_2)_n$-SH, BPn), (2) the desulfurized fragment (CH_3-C_6H_4-C_6H_4-$(CH_2)_n$, BPn-S), and (3) the methylbiphenyl fragment (CH_3-C_6H_4-C_6H_5 with m/z = 168). Comparison of the mass spectra taken for even-numbered BPn samples in the α phase and high-temperature phases β and δ as presented in Figure 2 exhibits pronounced differences in the emission of the complete molecule (BPn) and the desulfurized fragment (BPn-S). These differences are common to all three even-numbered BPn systems analyzed here and can be clearly identified looking at the abundance of the respective ions, that is, photoion signals normalized to the sum of all ions

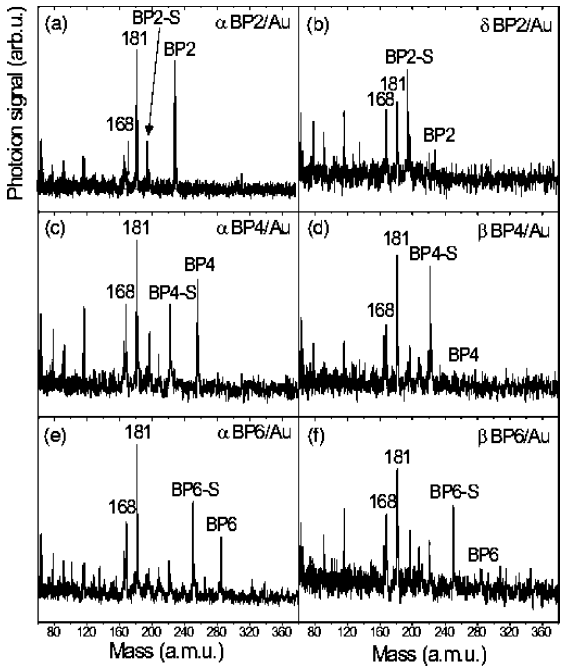

Figure 2. Photoionization mass spectra of neutral molecular fragments desorbed with low kinetic energy (~0.02 eV for particles with a mass of the order of 200 amu) during the 15-keV Ar^+ irradiation of BPn/Au(111) monolayers. (a) α-Phase BP2/Au(111), (b) δ-phase BP2/Au(111), (c) α-phase BP4/Au(111), (d) β-phase BP4/Au(111), (e) α-phase BP6/Au(111), (f) β-phase BP6/Au(111).

(Figure 3). The relative ion yield for the molecular fragment (Figure 3a) is lower for the high-temperature β/δ phases compared to the room temperature α phase, whereas the ratio is inverted for the desulfurized fragment (Figure 3b). In contrast to these two fragments where a clear-cut difference in the ion yield is observed for different phases across all even-numbered BPn, the picture for the CH_3-C_6H_4-C_6H_5 fragment (m/z = 168) is molecule-dependent. As seen from Figure 3c, the signal for BP2 is increased by the α → δ transition, whereas no difference between the phases is seen for BP4 and BP6. The change of phase affects not only the relative ion yields but also the total photoion signal. As shown in Figure 4, emission of neutral species from the α-phase SAMs is much more efficient compared to the emission obtained after bombarding high-temperature β/δ-phase SAMs.

All of these observations demonstrate that ion-induced emission of intact molecules and fragments is extremely sensitive to details of the structure and energetics of the SAMs. The data presented here show that not even a chemical change is required to alter the relative stability of the S−substrate and S−C bond against ion irradiation, and thus partial or complete removal of the SAM molecule, but just structural changes are sufficient. Most striking is, however, the fact that ion-induced desorption using a primary ion beam in the kiloelectronvolt energy range is so sensitive to these changes that are on a very different energy scale, that is, well below 1 eV.

This sensitivity is a consequence of the processes involved in ion-induced desorption where the high energy of the primary beam is distributed into different emission channels characterized by different kinetic energies. As mentioned briefly in the introduction, there is a high-energy channel of ballistically emitted particles that is expected to be insensitive to small rearrangements of molecules on the surface. It is, however, a second channel, which, as demonstrated in previous experiments,[9−12,28] is responsible for the overwhelming majority of parent molecules (BPn) and desulfurized fragments (BPn-S) to be emitted from

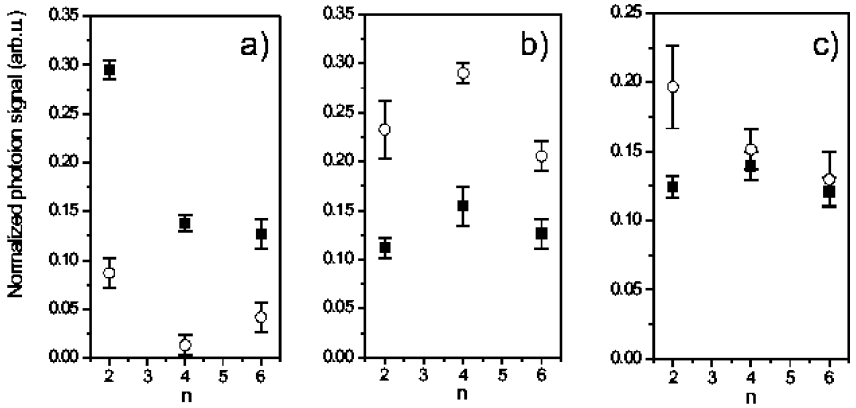

Figure 3. Photoion signal corresponding to (a) the parent molecules (BPn), (b) the desulfurized molecular fragment (BPn-S), and (c) fragment with $m/z = 168$ desorbed during the 15-keV Ar^+ irradiation of BPn/Au(111) with $n = 2$, 4, and 6. Relative intensities of the characteristic mass peaks are normalized to the total signal measured for a given BPn system. The filled symbols represent the signals for BP2/Au(111), BP4/Au(111), and BP6/Au(111) in α phase. The open symbols refer to signals for BP2/Au(111) in δ phase and BP4/6 on Au(111) in β phase.

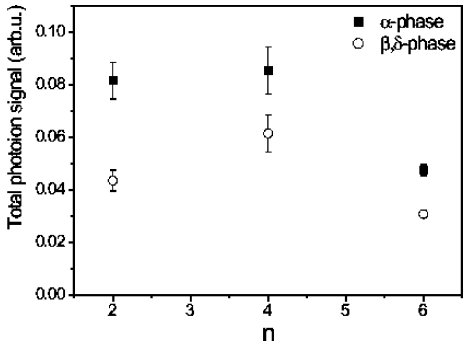

Figure 4. Total photoion signal of low-energy desorbed molecular fragments BPn/Au(111) during 15-keV Ar^+ irradiation. The filled symbols represent signals for BP2/Au(111), BP4/Au(111), and BP6/Au(111) in α phase. The open symbols refer to signals for BP2/Au in δ phase and BP4/Au(111) and BP6/Au(111) in β phase.

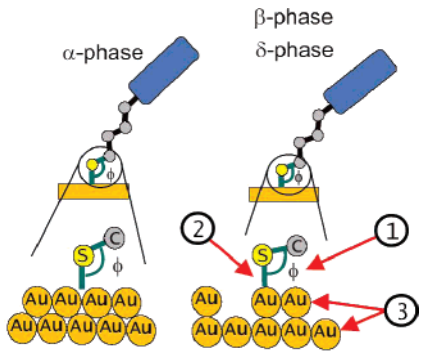

Figure 5. Schematic illustration of possible changes taking place at the Au−S−C interface during α → β and α → δ phase transitions in BPn ($CH_3(C_6H_4)_2(CH_2)_nSH$) SAMs with n = even chemisorbed on Au(111) substrate. Numbers 1, 2, and 3 indicate change in Au−S−C angle, adsorption site of S atom, and reconstruction of the Au(111) surface, respectively.

the monolayer at low thermal-like energies. Previous computer simulations indicated that gentle Au−S and S−C bond scission occurs following chemical reactions with reactive fragments such as radicals (H•) and other ionic and neutral fragments created by the impact of the primary ion.[29,30] This model of desorption by ion-induced chemical reactions and not by direct ballistic processes as assumed by others[13] is directly confirmed by the experiments presented here. Because the cross section for a chemical reaction depends, in general, critically on details of the electronic structure of reagents, steric conditions, and kinetic factors such as the activation energy, it can be understood that subtle changes in the structure of the BPn/Au(111) SAMs give rise to such pronounced changes in the emission yield and the fragmentation pattern.

We now take a brief look at the structural changes in BPn/Au(111) SAMs induced by phase transitions. For more details, we refer to our previous microscopic and spectroscopic studies.[25,26] In a simple qualitative model,[25] the occurrence of a phase transition depends on how the various factors, such as intermolecular interactions, coverage, and bonding configuration at the Au−S interface, enter into the energy balance of a SAM. In this model, the Au−S−C bending potential described by angle ϕ (see Figure 1) contributes significantly to the energetics of the SAM system whose stability depends on whether ϕ can be optimized along with or at the expense of other factors. Although the former, the cooperative way observed for odd-numbered BPn/Au(111) SAMs,[18,19] results in stable structures with ϕ adopting the preferred value, it is the latter, the competitive way observed for even-numbered BPn/Au(111), where ϕ has to deviate from the optimum due to restrictions set by the molecular structure and packing of the SAM. This competitive way gives rise to a variety of structures close in energy, and therefore preparation of even-numbered BPn/Au(111) SAMs at lower temperatures results in the metastable α phase, which can be transformed to the more stable β/δ phases upon annealing. The new structures of β and δ obtained for SAMs of BP4/BP6 and BP2 on Au(111) exhibit a lower packing density than the initial α phase. Because the strong S−Au bond makes the biggest contribution to the energy of the system, this reduction in density is energetically costly and must be compensated by other factors. Three of these factors seem to be of particular importance,[25] as illustrated in Figure 5. First, the larger distance between molecules permits that in the new phases the Au−S−C angle will achieve a value that is closer to the value of 104°, which is considered to be the preferred one for sulfur on Au(111).[31−33] Second, the phase transitions alter the arrangements of BPn molecules on the gold surface (different unit cells for corresponding structures). This results in changes in the adsorption sites of sulfur,[34,35] inducing a restructuring of the Au(111) surface,[36−38] and consequently affects the stability of the Au−S and S−C bonds. Third, the packing density is reduced, which, in combination with the two other factors, releases stress originating from the misfit between the structure preferred by the aromatic system and the Au(111) substrate.[39]

Having analyzed the features common to all even-numbered BPn/Au(111) SAMs, we close the discussion by turning to differences between these SAMs. It is clear from the experi-

mental evidence that BP2/Au(111) differs from BP4/Au(111) and BP6 on Au(111). When looking at changes in the relative photoion signals, it is clear from Figure 3 that the phase transition leads to a much more dramatic decrease in the parent molecule (Figure 3a) for BP2/Au(111) compared to BP4/Au(111) and BP6/Au(111). This is accompanied by a severe increase in the emission of the methylbiphenyl fragment ($m/z = 168$) after $\alpha \rightarrow \delta$ transition in BP2/Au(111), but for the same fragment no significant changes for the other two SAM systems (Figure 3c). These two observations can be straightforwardly linked to changes in the stability of the Au−S bond and the C−C bond between biphenyl and aliphatic parts of the molecule following structural changes induced by phase transitions. Because the SAMs of BP4 and BP6 on Au(111) have exactly the same final structure after phase transition ($\alpha \rightarrow \beta$), which is significantly different from the final structure of BP2/Au(111) ($\alpha \rightarrow \delta$), the observed differences fully support the relation between the details in the film structure of the molecular overlayer and the ion-induced desorption. Moreover, a significant change in the efficiency of the ion-induced scission of the C−C bond between the biphenyl and aliphatic parts observed only after $\alpha \rightarrow \delta$ transition in BP2 SAMs can be associated with the reorientation of the herringbone arrangement of biphenyl moieties[26] observed only upon this phase transition.

In conclusion, the study of ion-induced desorption from a homologue series of BPn SAMs on Au(111) in different phases evidences for the first time a striking sensitivity of Au−S and S−C bond cleavage to only structural, and not chemical, changes at the SAM−substrate interface. This shows that ion-induced desorption is much more sensitive to details of a SAM system than one would expect from the high energies of the primary ions. Such a sensitivity directly confirms a previous molecular simulation-based model of SAM desorption by ion-induced chemical reactions, which, if true, should depend on the details of the spatial and electronic configuration of the chemical bonds terminated during the desorption process. Furthermore, in light of the analytical capabilities of this technique, subtle changes at the buried SAM−substrate interface can be revealed that are very difficult to assess with other surface-sensitive techniques. With respect to applications of SAMs in ion beam lithography, the present experiments clearly demonstrate that exact control of the SAM structure and the SAM−substrate interface is required to optimize the complete removal of molecular species. It still remains very difficult, if possible at all, to describe in detail the relation between the electronic structure of the given bond and the probability of its scission by ion-induced chemical reactions and thus to give an exact recipe for SAM structures suitable for lithographic applications.

Acknowledgment. This work is financially supported by the Belgian Fund for Scientific Research − Flanders (FWO), the Flemish Concerted Research Action (GOA) Program, and the Belgian Interuniversity Poles of Attraction (IAP) Program. P.C greatly acknowledges the program *Homing* by the Foundation for Polish Science and an Adam Krzyżanowski Stipend at the Jagiellonian University. Z.P acknowledges support by the N204 4097 33 program. M.B. acknowledges support by EPSRC.

Supporting Information Available: Sample preparation and experimental setup. This material is available free of charge via the Internet at http://pubs.acs.org.

References and Notes

(1) Smith, R. K.; Lewis, P. A.; Weiss, P. S. *Prog. Surf. Sci.* **2004**, *75*, 1−68.

(2) Love, J. C.; Estroff, L. A.; Kriebel, J. K.; Nuzzo, R. G.; Whitesides, G. M. *Chem. Rev.* **2005**, *105*, 1103−1170.

(3) Zharnikov, M.; Grunze, M. *J. Vac. Sci. Technol., B* **2002**, *20*, 1793−1807.

(4) Sun, S. Q.; Leggett, G. J. *Nano Lett.* **2004**, *4*, 1381−1384.

(5) Bard, A.; Berggren, K. K.; Wilbur, J. L.; Gillaspy, J. D.; Rolstone, S. L.; McClelland, J. J.; Phillips, W. D.; Prentiss, M.; Whitesides, G. M. *J. Vac. Sci. Technol., B* **1997**, *15*, 1805−1810.

(6) Ada, E. T.; Hanley, L.; Etchin, S.; Melngalis, J.; Dressick, W. J.; Chen, M. S.; Calvert, J. M. *J. Vac. Sci. Technol., B* **1995**, *13*, 2189−2196.

(7) Li, C.; Zhang, D. H.; Liu, X. L.; Han, S.; Tang, T.; Zhou, C. W.; Fan, W.; Koehne, J.; Han, J.; Meyyappan, M.; Rawlett, A. M.; Price, D. W.; Tour, J. M. *Appl. Phys. Lett.* **2003**, *82*, 645−647.

(8) Wong, S. C. C.; Lockyer, N. P.; Vickerman, J. C. *Surf. Interface Anal.* **2005**, *37*, 721−730.

(9) Riederer, D. E.; Chatterjee, R.; Rosencrance, S. W.; Postawa, Z.; Dunbar, T. D.; Allara, D. L.; Winograd, N. *J. Am. Chem. Soc.* **1997**, *119*, 8089−8094.

(10) Cyganik, P.; Postawa, Z.; Meserole, C. A.; Vandeweert, E.; Winograd, N. *Nucl. Instr. Methods Phys. Res., Sect. B* **1999**, *148*, 137−142.

(11) Postawa, Z.; Meserole, C. A.; Cyganik, P.; Szymonska, J.; Winograd, N. *Nucl. Instr. Methods Phys. Res., Sect. B* **2001**, *182*, 148−154.

(12) Cyganik, P.; Vandeweert, E.; Postawa, Z.; Bastiaansen, J.; Vervaecke, F.; Lievens, P.; Silverans, R. E.; Winograd, N. *J. Phys. Chem. B* **2005**, *109*, 5085−5094.

(13) Chenakin, S. P.; Heinz, B.; Morgner, H. *Surf. Sci.* **1999**, *421*, 337−352.

(14) Pacholski, M. L.; Cannon, D. M.; Ewing, A. G.; Winograd, N. *J. Am. Chem. Soc.* **1999**, *121*, 4716−4717.

(15) Zharnikov, M.; Frey, S.; Rong, H.; Yang, Y. J.; Heister, K.; Buck, M.; Grunze, M. *Phys. Chem. Chem. Phys.* **2000**, *2*, 3359−3362.

(16) Rong, H. T.; Frey, S.; Yang, Y. J.; Zharnikov, M.; Buck, M.; Wühn, M.; Wöll, C.; Helmchen, G. *Langmuir* **2001**, *17*, 1582−1593.

(17) Heister, K.; Rong, H. T.; Buck, M.; Zharnikov, M.; Grunze, M.; Johansson, L. S. O. *J. Phys. Chem. B* **2001**, *105*, 6888−6894.

(18) Azzam, W.; Cyganik, P.; Witte, G.; Buck, M.; Wöll, C. *Langmuir* **2003**, *19*, 8262−8270.

(19) Cyganik, P.; Buck, M.; Azzam, W.; Wöll, C. *J. Phys. Chem. B* **2004**, *108*, 4989−4969.

(20) Long, Y. T.; Rong, H. T.; Buck, M.; Grunze, M. *J. Electroanal. Chem.* **2002**, *524*, 62−67.

(21) Thom, I.; Buck, M. *Surf. Sci.* **2005**, *581*, 33−46.

(22) Felgenhauer, T.; Rong, H. T.; Buck, M. *J. Electroanal. Chem.* **2003**, *550*, 309−319.

(23) Frey, S.; Rong, H. T.; Heister, K.; Yang, Y. J.; Buck, M.; Zharnikov, M. *Langmuir* **2002**, *18*, 3142−3150.

(24) Cyganik, P.; Buck, M. *J. Am. Chem. Soc.* **2004**, *126*, 5960−5961.

(25) Cyganik, P.; Buck, M.; Strunskus, T.; Shaporenko, A.; Wilton-Ely, J. D. E. T.; Zharnikov, M.; Wöll, C. *J. Am. Chem. Soc.* **2006**, *128*, 13868−13878.

(26) Cyganik, P.; Buck, M.; Strunskus, T.; Shaporenko, A.; Witte, G.; Zharnikov, M.; Wöll, C. *J. Phys. Chem. C* **2007**, *111*, 16909−16919.

(27) Lüssem, B.; Müller-Meskamp, L.; Karthäuser, S.; Homberger, M.; Simon, U.; Waser, R. *J. Phys. Chem. C* **2007**, *111*, 6392−6397.

(28) Vandeweert, E.; Bastiaansen, J.; Vervaecke, F.; Lievens, P.; Silverans, R. E.; Cyganik, P.; Postawa, Z.; Rong, H. T.; Buck, M. *Appl. Phys. Lett.* **2003**, *82*, 1114−1116.

(29) Taylor, R. S.; Garrison, B. J. *Int. J. Mass. Spectrom.* **1995**, *143*, 225−233.

(30) Chatterjee, R.; Postawa, Z.; Winograd, N.; Garrison, B. J. *J. Phys. Chem. B* **1999**, *103*, 151−163.

(31) Sellers, H.; Ulman, A.; Shnidman, Y.; Eilers, J. E. *J. Am. Chem. Soc.* **1993**, *115*, 9389−9401.

(32) Krüger, D.; Fuchs, H.; Rousseau, R.; Marx, D.; Parrinello, M. *J. Chem. Phys.* **2001**, *115*, 4776−4786.

(33) Yourdshahyan, Y.; Rappe, A. M. *J. Chem. Phys.* **2002**, *117*, 825−833.

(34) Nara, J.; Higai, S.; Morikawa, Y.; Ohno, T. *J. Phys. Chem. B* **2004**, *120*, 6705−6711.

(35) Gottschalck, J.; Hammer, B. *J. Chem. Phys.* **2002**, *116*, 784−790.

(36) Molina, L. M.; Hammer, B. *Chem. Phys. Lett.* **2002**, *360*, 264−271.

(37) Maksymovych, P.; Sorescu, D. C.; Yates, J. T. *Phys. Rev. Lett.* **2006**, *97*, 146103.

(38) Yu, M.; Bovet, N.; Satterley, C. J.; Bengio, S.; Lovelock, K. R. J.; Milligan, P. K.; Jones, R. G.; Woodruff, D. P.; Dhanak, V. *Phys. Rev. Lett.* **2006**, *97*, 166102.

(39) Cyganik, P.; Buck, M.; Wilton-Ely, J. D.; Wöll, C. *J. Phys. Chem. B* **2005**, *109*, 10902−10908.